

Impact of Direct Ageing on Mechanical Properties and Residual Stresses of Maraging 300 Steel Manufactured by SLM

R. Halama^{1,a}, M. Kořínek¹, J. Čapek², K. Trojan², J. Hajnyš¹

¹ VŠB-Technical University of Ostrava, 17. listopadu 2172/15, 708 00 Ostrava-Poruba, Czech Republic

² Czech Technical University in Prague, Trojanova 13, 120 00 Prague, Czech Republic

^a radim.halama@vsb.cz

Abstract: This paper describes the main results of research conducted on samples manufactured by selective laser melting of maraging steel 300 powder. The results of the tensile tests helped us to construct maps of yield and ultimate strength as a function of temperature and time hold of direct ageing of the material. Furthermore, X-ray diffraction was used to determine the decrease of residual stresses with time during heat treatment under the lowest temperature. The magnitude of residual stresses in the axial direction of the sample was reduced by 60% by heat treatment.

Keywords: additive manufacturing; residual stresses; X-ray diffraction; maraging steel; heat treatment.

1 Introduction

Selective laser melting (SLM) is a technology that falls into the group of additive manufacturing (AM). SLM is a promising technique for consolidating metal powder and presents a plethora of opportunities for the creation of parts. Using a scanning energy source, it entails selectively melting sections of a thin, flat powder bed layer by layer (20–100 μm thick) to create 3D parts [1]. Complex residual stresses (RS) distribution is produced during the SLM process when regions are heated in accordance with the scan method, allowing parts to heat and cool independently. The application of heat treatment (HT) prior to removing the part from the build plate and removing supports is an efficient approach to reduce RS in printed parts. To prevent microstructural alterations, the temperature for HTs must be carefully chosen; otherwise, the high strength of the material may be lost.

The maraging steel 300 (1.2709 or MS300) has high strength, excellent toughness, and weldability, is based on precipitation hardening and ranks among a nickel-iron alloy. The reason for the increased strength of maraging steel is that the intermetallic nanoparticles $\text{Ni}_3(\text{Mo}, \text{Ti})$ and Fe_2Mo precipitate during ageing [2]. Steel is used extensively in the automobile, aerospace and tooling industries [3]. To modify the microstructure and improve the mechanical properties, conventional HT is commonly applied after printing by the SLM method. The HT usually consists of solution treatment, solution ageing, and direct ageing [4, 5]. In recent years, several studies have been conducted on maraging steels and their HT. The results show that in the as-built condition, the tensile strength values are around 1200 MPa and the ductility is 12% [6]. Applying direct ageing at 480°C and ageing for 5 h, the ultimate tensile strength values of 2217 MPa can be achieved [7]. When combining both HTs, namely solution treatment at 820°C for 1 h and ageing at 460°C for 5 h, the ultimate tensile strength of 2033 MPa was obtained, as the tensile ductility decreased from 10% to 5% [8].

The impact of direct ageing at various temperatures and different holding times on the mechanical properties of MS300 samples prepared with SLM has been reported in a preliminary study [9]. In this contribution, we precise the results of mechanical properties from new tensile tests and the impact of HT on residual stresses in vertically printed specimens made of MS300 is investigated

2 Material and Methods

2.1 Parameters of Additive Manufacturing Process

The standard chemical content of the metallic powder is available in the product data sheet [10]. All specimens for mechanical testing were printed using the Renishaw AM500E SLM printer. The print of the specimens was done in the Z direction, which is the vertical orientation of the specimen axis. Table 1 lists the primary printing parameters that are used in the AM process. To avoid oxidation, argon with a purity of 5.0 was poured into the chamber during production. To reduce residual stresses in the AM process, the building platform was heated to 170°C.

Tab. 1: Printing parameters used in the SLM process.

3D printing strategy	Laser power [W]	Laser rate [mm · s ⁻¹]	Layer thickness [μm]
“meander”	400	650	40

2.2 Postprocessing

In this study, we present new results from tensile tests considering HT: 490°C, 520°C, 840°C, 900°C (always 1, 2, 6, and 10 hours). A chamber furnace LH 120/12 from Nabertherm GmbH was used for the heat treatment of the tested samples. This furnace has a power of 12 kW and reaches temperatures of up to 1200°C. Individual samples were placed in the oven for a predetermined time and temperature. The initial temperature was 22°C, from which it increased to a predetermined temperature at a rate of 600°C/h. After the given temperature was reached, there was a holding time at the heat treatment temperature. After the holding time had elapsed, the samples were withdrawn, and cooling continued slowly in the air.

2.3 Tensile Testing

All tensile tests were performed using the LabControl 100 kN / 1000 Nm hydraulic testing machine. The diameter of the round sample was 5 mm and the length of the straight part was 40 mm. The position rate applied in all tests was 10 mm/min. For each HT, the tensile test was performed three times, while for one sample, the Epsilon Tech 3560 biaxial extensometer was used to obtain information on the transverse strain. The disadvantage of the extensometer is the short gauge length (10 mm). Necking usually occurred outside of the measured area. Therefore, the ductility from such tests is not included in the overall evaluation. In all other tests, the axial strain was measured by digital image correlation (2×2.3Mpx CCD cameras, Alpha X-Sight software).

2.4 Residual Stress Determination

X-ray diffraction measurements to obtain RS were done on samples subjected to HT at 490°C. Macroscopic RS were determined from the circumference of the samples in the axial direction samples. The RS values were calculated from lattice deformations determined on the basis of experimental dependencies of $2\theta(\sin^2\psi)$ assuming a biaxial state of residual stress (θ is the diffraction angle, ψ the angle between the sample surface and the diffracting lattice planes). The diffraction angle was determined as the centre of gravity of the $\text{CrK}\alpha_{1,2}$ doublet diffracted by the lattice planes $\{211\}$ of the α -Fe phase. The X-ray elastic constants $\frac{1}{2}s_2 = 5.76 \text{ TPa}^{-1}$, $s_1 = -1.25 \text{ TPa}^{-1}$ were used for the stress calculation. The experimental error is the standard deviation according to the “ $\sin^2\psi$ ” residual stress calculation algorithm.

3 Results

3.1 Mechanical Tests

The resulting mechanical properties are presented in the form of characteristic engineering stress-strain curves for particular HTs in Fig. 1a. For a comparison, contour maps are presented in Figs. 1b-d. There are two local extrema in the map of yield strength and ductility evaluated from tensile tests on heat treated samples, see Figs. 1b,c. The highest ultimate strength is obtained from the temperature of 490°C and 10 hours (Fig. 1d).

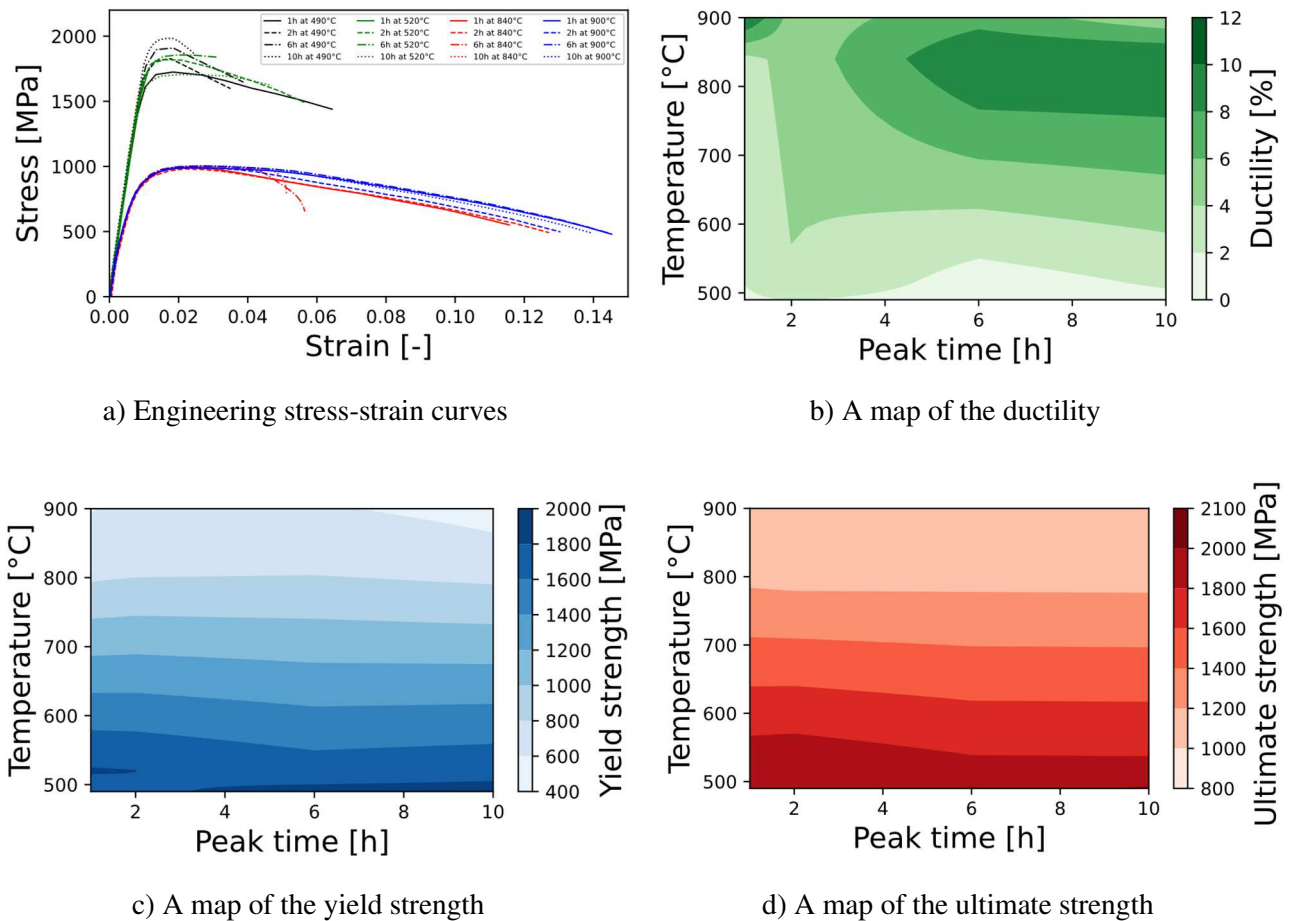


Fig. 1: Results of mechanical tests on MS300 manufactured by SLM with specific HTs.

3.2 Residual Stresses

The temperature of 490°C was selected for the investigation of averaged RS analyzed by X-ray diffraction around the circumference of MS300 in the axial direction as a function of hold time (Fig. 2). All analyzed samples showed tensile residual stresses. As the annealing time increased while maintaining the same temperature, the average tensile residual stress of the test specimens decreased. When the time was increased to five times, there was a decrease in residual stresses by about 60%. This observation is not surprising since the degree of residual stress redistribution is a function of temperature and time. Since there was a continual decrease in adverse tensile stresses with increasing annealing time, it is not surprising that the specimen annealed at a temperature of 490°C for 10 hours exhibited the highest ultimate strength. The residual stresses add to the applied stresses and when the tensile residual stresses dominate the surface, there is effectively a reduction in ultimate strength.

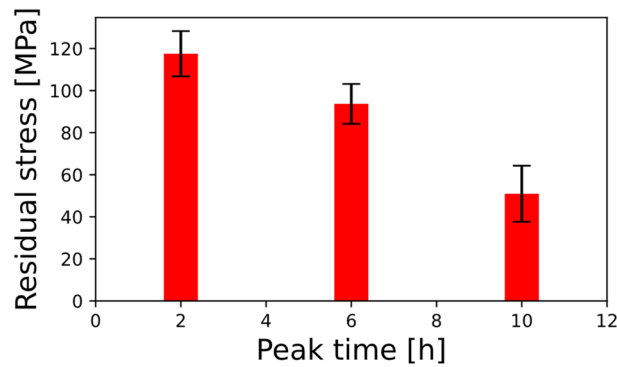


Fig. 2: Results of residual stress on MS300 SLM resulting from HTs.

4 Conclusion

In total, sixteen HT conditions, as a combination of four temperatures and four time holds, have been investigated in this study conducted on MS300. The best case from the strength increase point of view has been selected for the evaluation of the decrease in RS due to HT. The magnitude of the axial component of residual stresses decreased to 40% of its initial value. The findings of the study indicate that RS cannot be completely eliminated by 10 hours of classic direct aging. However, the specimen with the lowest tensile residual stresses exhibited the highest ultimate strength. A technique using uneven cooling developed for AlSi10Mg [11] can eventually help to reduce residual stresses in printed components.

Acknowledgement

This work is an output of the project with financial support from the Czech Science Foundation under registration no. 23-04724S. The work of CTU staff was supported by the Grant Agency of the Czech Technical University in Prague, grant No. SGS22/183/OHK4/3T/14.

References

- [1] R. Halama et al., Cyclic plasticity of additively manufactured metals, in book: *Cyclic Plasticity of Metals: Modeling Fundamentals and Applications*, Amsterdam, Elsevier, 2022, 397–433, <https://doi.org/10.1016/B978-0-12-819293-1.00022-X>.
- [2] T. Allam et al., Tailoring the nanostructure of laser powder bed fusion additively manufactured maraging steel, *Additive Manufacturing* 36 (2020) 101561, <https://doi.org/10.1016/j.addma.2020.101561>.
- [3] E.-A. Jagle et al., Precipitation and austenite reversion behavior of a maraging steel produced by selective laser melting. *Journal of Materials Research* 29 (2014) 2072–2079, <https://doi.org/10.1557/jmr.2014.204>.
- [4] Y. Bai et al., Effect of heat treatment on the microstructure and mechanical properties of maraging steel by selective laser melting, *Materials Science and Engineering* 760 (2019) 105–117, <https://doi.org/10.1016/j.msea.2019.05.115>.
- [5] J. Song et al., Effect of heat treatment on microstructure and mechanical behaviours of 18Ni-300 maraging steel manufactured by selective laser melting, *Optics & Laser Technology* 120 (2019) 105725, <https://doi.org/10.1016/j.optlastec.2019.105725>.
- [6] J. Suryawanshi et al., Tensile, fracture, and fatigue crack growth properties of a 3D printed maraging steel through selective laser melting, *Journal of Alloys and Compounds* 725 (2017) 355–364, <https://doi.org/10.1016/j.jallcom.2017.07.177>.

- [7] K. Kempen et al., Microstructure and mechanical properties of selective laser melted 18Ni-300 steel, *Physics Procedia* 12 (2011) 255–263, <https://doi.org/10.1016/j.phpro.2011.03.033>.
- [8] J. Mutua et al., Optimization of selective laser melting parameters and influence of post heat treatment on microstructure and mechanical properties of maraging steel. *Materials & Design* 139 (2018) 486–497, <https://doi.org/10.1016/j.matdes.2017.11.042>.
- [9] A. Kvita, Research into the Influence of Heat Treatment on the Mechanical Properties of the MS300 Material Produced by the SLM Method, Diploma thesis, Ostrava, Faculty of Mechanical Engineering, VŠB-TU Ostrava, 2022. (in Czech)
- [10] Maraging steel M300 powder for additive manufacturing, RENISHAW [online], [cit. 2024-05-21], available at: <https://www.renishaw.com>.
- [11] C. H. Lim et al., Novel method of residual stress reduction for AISi10Mg manufactured using selective laser melting without compromise of mechanical strength, *Virtual and Physical Prototyping* 18 (2022) e2131583, <https://doi.org/10.1080/17452759.2022.2131583>.